Displacement of the Lamina Cribrosa in Response to Acute Intraocular Pressure Elevation in Normal Individuals of African and European Descent

Massimo A. Fazio,[1,2] John K. Johnstone,[3] Brandon Smith,[1] Lan Wang,[1] and Christopher A. Girkin[1]

[1]Department of Ophthalmology, University of Alabama at Birmingham, Birmingham, Alabama, United States
[2]Department of Biomedical Engineering, University of Alabama at Birmingham, Birmingham, Alabama, United States
[3]Department of Computer and Information Sciences, University of Alabama at Birmingham, Birmingham, Alabama, United States

Correspondence: Christopher A. Girkin, Department of Ophthalmology, Chief Medical Officer, Callahan Eye Hospital, University of Alabama at Birmingham, AL 35233, USA; cgirkin@uab.edu.

Submitted: August 12, 2015
Accepted: May 24, 2016

Citation: Fazio MA, Johnstone JK, Smith B, Wang L, Girkin CA. Displacement of the lamina cribrosa in response to acute intraocular pressure elevation in normal individuals of African and European descent. *Invest Ophthalmol Vis Sci*. 2016;57:3331–3339. DOI:10.1167/iovs.15-17940

Purpose. To assess if the in vivo mechanical displacement of the anterior laminar cribrosa surface (ALCS) as a response of an acute elevation in intraocular pressure (IOP) differs in individuals of European (ED) and African descent (AD).

Methods. Spectral-domain optical coherence tomography (SDOCT) scans were obtained from 24 eyes of 12 individuals of AD and 18 eyes of 9 individuals of ED at their normal baseline IOP and after 60 seconds IOP elevation using ophthalmodynamometry. Change in depth (displacement) of the LC and to the prelaminar tissue (PLT) were computed in association with the change (delta) in IOP (Δ IOP), race, age, corneal thickness, corneal rigidity (ocular response analyzer [ORA]), and axial.

Results. In the ED group for small IOP elevations (Δ IOP $<$ 12 mm Hg), the ALCS initially displaced posteriorly but for larger increase of IOP an anterior displacement of the lamina followed. Inversely, in the AD group the ALCS did not show a significant posterior displacement for small Δ IOP, while for larger IOP increases the ALCS significantly displaced posteriorly. Posterior displacement of the lamina cribrosa (LC) was also significantly correlated with longer axial length, higher corneal thickness, and ORA parameters. Prelaminar tissue posteriorly displaced for any magnitude of Δ IOP, in both groups.

Conclusions. The African descent group demonstrated a greater acute posterior bowing of the LC after adjustment for age, axial length, Bruch's membrane opening (BMO) area, and ORA parameters. Greater PLT posterior displacement was also seen in the AD group with increasing IOP, which was tightly correlated with the displacement of the LC.

Keywords: lamina cribrosa, optic nerve, optic disc, optical coherence tomography, optic nerve head

The lamina cribrosa (LC) provides structural and functional support to the retinal ganglion cell (RGC) axons as they pass from the relatively high-pressure environment within the eye to a lower pressure region in the retrobulbar cerebrospinal space. This structure experiences significant mechanical strain at all levels of intraocular pressure (IOP)[1,2] and is thought to play a critical role in the development of axonal injury with glaucoma.[3–7] Variation in the material properties and morphology of the lamina cribrosa and sclera will affect its mechanical response to the loading force of IOP,[8] and these parameters may play a significant role in individual susceptibility to glaucoma.[4,9–12]

The relatively recent advent of enhanced depth imaging in spectral-domain optical coherence tomography (EDI-SDOCT),[13] swept-source optical coherence tomography (SS-OCT), b-scans shadow-removal[14] postprocessing, and light attenuation compensation[15] algorithms has enabled the visualization of some of these laminar morphologic changes in vivo.[16] Thus, we can now investigate the relationship between alterations in the morphology of the lamina cribrosa and progression along with its complex relationship with other known risk factors, in vivo.

The lamina cribrosa position has been shown to change with the development of glaucoma,[17,18] with normal aging, and across racial groups, with a more posterior position of the LC with age in individuals of African descent (AD) compared to those of European descent (ED).[19] Further, using confocal scanning laser tomography and SDOCT the lamina cribrosa has been shown to shift in position with acute elevation of IOP,[8,20–22] which could be used as a potential in vivo measure of the biomechanical behavior of the LC. These prior compliance studies have all been performed in populations of ED, and no studies have been performed in AD individuals in which significant variation in optic nerve[19] and scleral morphology[23] and material properties[24,25] have been demonstrated. These morphological and biomechanical racial differences may, in part, play a role in the greater susceptibility to glaucoma seen in the AD population experienced at all levels of IOP.[26,27] The principal aim of this work was to test the hypothesis that the IOP-induced acute laminar displacement is different in donors of ED and AD and to determine the relevant factors associated with shifts in laminar position across racial groups. To accomplish this, we quantified the optic nerve head

This work is licensed under a Creative Commons Attribution-NonCommercial-NoDerivatives 4.0 International License.

Downloaded From: http://iovs.arvojournals.org/pdfaccess.ashx?url=/data/journals/iovs/935339/ on 07/31/2017

(ONH) principal surfaces displacements for an acute increase of IOP in normal patients.

Materials and Methods

Participants enrolled in this study were part of a National Institutes of Health–funded cohort study conducted at the University of Alabama at Birmingham: the African Descent and Glaucoma Evaluation Study (ADAGES). Only subjects without evidence of ocular diseases that would affect the optic nerve, retina, or choroid, as defined below, were invited to participate. The participants were consented to the additional study. The University of Alabama at Birmingham institutional review board approved the study methods that adhered to the tenets of the Declaration of Helsinki.

Each participant underwent a complete ophthalmological exam that included medical history, Snellen best-corrected visual acuity, Early Treatment Diabetic Retinopathy Study (ETDRS) visual acuity, color vision, slit-lamp biomicroscopy, applanation tonometry for IOP, central corneal thickness (CCT) measurement, axial length (AL) measurement, dilated funduscopy, stereoscopic ophthalmoscopy of the optic disc, and stereoscopic fundus photography. Standard Swedish Interactive Thresholding Algorithm 24-2 perimetry was performed to define normality for inclusion in this study (see below). Additionally, all subjects underwent testing with the ocular response analyzer (ORA) to obtain measurements of corneal hysteresis (CH) and corneal resistance factor (CRF) preceding baseline EDI-SDOCT imaging for the compliance testing.

Inclusion/Exclusion Criteria

Participants were older than 18 years of age. Eligible participants had open iridocorneal angles, a best-corrected acuity of 20/40 or better, and refractive error ± 5.0 diopters sphere and ± 3.0 diopters cylinder. Patients with diabetes and any retinal, corneal, or optic nerve disease were excluded. A family history of glaucoma was allowed. Participants were excluded if they had a history of intraocular surgery (except for uncomplicated cataract surgery), elevated IOP (> 22 mm Hg) at the time of the study, a history of elevated IOP, prior use of glaucoma medication, other intraocular eye disease, or other diseases affecting visual field (e.g., pituitary lesions, demyelinating diseases, human immunodeficiency virus positive or acquired immune deficiency syndrome). Further, patients were excluded if there was a diagnosis of Alzheimer's disease, Parkinson's disease, or previous brain injury including stroke, psychoses, or other neurological or psychiatric conditions that would prevent participation in a psychophysical test.

We required two reliable tests (less than 25% fixation losses, false negatives, and false positives) on 24-2 standard automated perimetry (Carl Zeiss Meditec, Dublin, CA, USA) using the Swedish interactive threshold algorithm in both eyes at baseline for inclusion in the study. Reliability was defined as $< 33\%$ false positives, false negatives, and fixation losses. A field was considered normal if the pattern standard deviation was not triggered at 5% or less, the Glaucoma Hemifield Test was within normal limits, and the field showed no sign of glaucomatous defect based on subjective evaluation from the enrolling clinician. The optic nerves were assessed by stereoscopic photos by a fellowship-trained glaucoma specialist. Subjects with any structural finding suggestive of glaucoma (i.e., notching, rim thinning, disc hemorrhages, or retinal nerve fiber layer defects as judged) were excluded.

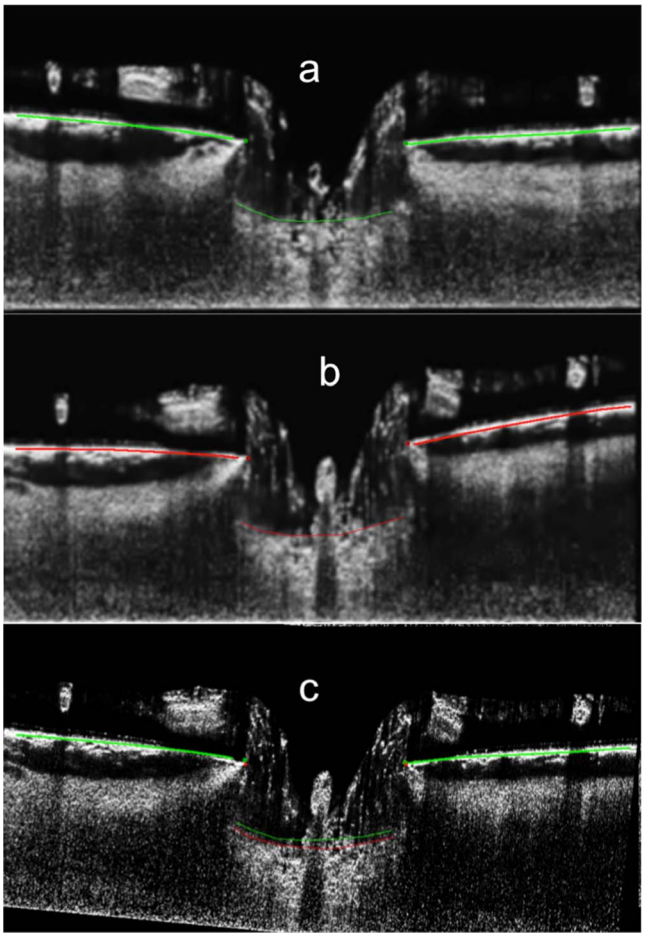

Figure 1. Simplified representation of the morphological changes in ALCS depth visible in a comparison of the same radial b-scan before (**a**) and after (**b**) the IOP elevation. A variation of the LC is visible with the superimposition of the reference (*green*) and elevated (*red*) IOP b-scans, respectively (**c**).

Compliance Testing: Acute IOP Elevation and SDOCT Image Acquisition Protocol

Twenty-four eyes of 12 individuals of AD and 18 eyes of 9 individuals of ED underwent ocular mechanical compliance testing, as follows. Baseline IOP measurement was obtained using a tonopen. Baseline EDI-SDOCT imaging of the optic nerve was performed prior to IOP elevation with the Spectralis OCT (Heidelberg Engineering; Family Acquisition Module 5.4.8.0) with 24 radial scans centered on the center of the optic nerve head using enhanced depth imaging.[28] Scans were evaluated for imaging quality by the operator, and images were re-acquired if there was improper b-scan positioning in the imaging frame, a quality score < 20, or poor centration of the optic nerve head. Radial scans were acquired using a signal averaging of nine b-scans. A sample of the effect of the acute IOP elevation is reported in Figure 1. For visualization purposes, the Bruch's membrane in the b-scan acquired at elevated IOP (Fig. 1b) is used as a reference line to align the scan at the reference IOP (Fig. 1a); from the superimposition of anterior lamina cribrosa surface (ALCS) outline at reference- and high-pressure, it is noticeable the shift of the ALCS caused by the IOP elevation (Fig. 1c). It is important to note that the 3D quantification method used in this study and described in the next paragraph does not require an alignment to the b-

Investigative Ophthalmology & Visual Science

Downloaded From: http://iovs.arvojournals.org/pdfaccess.ashx?url=/data/journals/iovs/935339/ on 07/31/2017

scans to the BM plane, and that the ALCS depth variation is estimated in the actual 3D space and not the 2D image plane.

In order to induce a temporary elevation of the IOP, a compressive force of approximately 35 Pa on the inferior temporal globe was applied by means of an ophthalmodynamometer, in a similar manner described by Agoumi et al.[22] This compressive force caused increase in IOP of approximately 14 mm Hg and did not visibly disturb OCT image quality. Compression was maintained while the following steps were performed: 60 seconds waiting time allowing short-time mechanical effects of the tissue to be minimized; an EDI-SDOCT scan was re-acquired in a similar manner to baseline testing; IOP measurement was re-performed with a tonopen to estimate the actual increase of pressure. After these steps, the ophthalmodynamometer compression was removed. The total time of IOP elevation was approximately 2 minutes. After 5 minutes following initial IOP elevation, an additional measurement of IOP was performed.

EDI-SDOCT Image Processing and Quantification

In order to enhance the visibility of the deeper tissue, all b-scans from the EDI-SDOCT volumes were postprocessed using adaptive light attenuation compensation,[29,30] in order to increase a clearer visualization of the lamina cribrosa. Light attenuation compensated scan volumes were then loaded in a custom software developed for 3D delineation of histologic and OCT data that has been described in prior publications[31,32] based on the Visualization Toolkit (VTK, Clifton Park, NY, USA). A trained observer masked to subject characteristics manually delineated the internal limiting membrane (ILM), BMO, inner and outer choroidal layers, and the anterior surface of the LC in 24 equally spaced radial sections of each OCT scan. Laminar visibility was variable among individuals. An average of 202 points (range, 23–534) were used to define the LC anterior surface. Considering that former studies observed significant differences in the ONH morphology of ED and AD for all the OCT scans, the area of the 3D surface representing the delineated inner laminar surface was estimated. Differences in laminar visibility by race and IOP elevation were assessed and reported in the Results section.

Computing Laminar and Prelaminar Tissue (PLT) Depth

Depth of the ALCS was measured both from a BMO and scleral reference plane.[33] Since the difference in ALCS position seen with IOP elevation was independent of the chosen reference plane, the commonly used BMO reference plane-based measures were used for the present analysis. This similarity between reference planes is possibly due to the lack of significant change in choroidal thickness with the acute increase of IOP ($P = 0.94$).[19] Since the BMO is nearly planar, its best-fitting plane, computed through principal component analysis of the BMO samples, can serve as a reference plane. The depth of a laminar point is its distance from this BMO plane, positive only on the laminar side of the BMO plane. Laminar depth is sampled across a reconstruction of the lamina, leading to a computation of mean laminar depth, as follows. To build a uniform sampling of the LC sections, each section is downsampled (while preserving shape, using the Douglas-Peucker decimation algorithm), interpolated by a B-spline curve, then uniformly sampled. An optimal triangle mesh is built from this uniform sampling of the LC sections (using the classic contour reconstruction algorithm of Song et al.[34]). The centroids of each triangle of this mesh are found, and the laminar depth at each centroid is measured (its distance from the BMO plane).

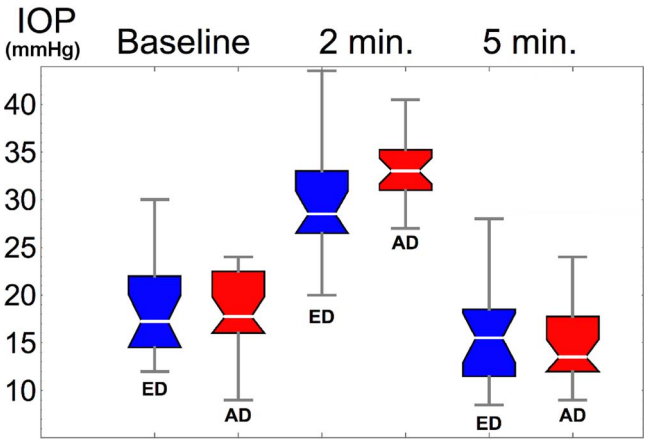

FIGURE 2. Box-and-whisker plots of the IOP distributions for the ED (*blue*) and AD (*red*) individuals. Morphological parameters here reported correspond to the baseline IOP and after 2 minutes (min.) of the ophthalmodynamometry.

Mean laminar depth is now a weighted linear combination of these centroid depths and weighted by triangle area (weight = triangle area / mesh area) in order to achieve a standardized quantification independent of the number of sampling points used for the definition of the laminar surface morphology. Indeed, this simulates a uniform sampling of depth across the surface.[19]

Prelaminar tissue depth is computed analogously. The prelaminar tissue depth of a point of the ILM is its distance from the BMO reference plane. As with laminar depth, a mesh is constructed and depths are sampled across this mesh to calculate the mean depth of the ILM. For prelaminar tissue depth, measurements are constrained to the cylinder above the best-fitting ellipse of the BMO. Prelaminar tissue depth was quantified based on distance from the BMO reference plane to the surface of the manually delineated ILM. As with laminar depth, a mesh was constructed and depths were sampled uniformly across this mesh to calculate the depth of the ILM. Measurements were constrained to the cylinder above the best-fitting ellipse of the BMO. Prelaminar tissue depth is positive on the laminar side of the BMO plane, otherwise negative. The methods for computing ALCS and PLT depth are described in detail in a prior publication.[19,33] In order to assess the dependency of the measurements from the interrater variability, we assessed the Bland-Altman limit-of-agreement and the intraclass correlation coefficient (ICC) for the laminar depth measurement. For that purpose, 12 OCT scans were manually delineated from both raters, and laminar depth was computed using the quantification method described in the previous paragraph. A Bland-Altam plot reporting the limit-of-agreement (18 μm, 95% confidence interval [CI]) for the mean laminar depth estimated by the two raters is shown in Figure 3 (left). In right plot of Figure 3, it can be noticed that the magnitude of disagreement was correlated (Pearson = 0.62) with the magnitude of the measurement that invalidates the interpretation of the limit-of-agreement as an estimate of the interrater variability.[35] The lower agreement between raters observed for shallow laminae and a higher agreement for deeper laminae were plausibly imputable to the lamina visibility change as a function of mean depth; a higher amount of PLT present in shallower ONHs would diminish the visibility of the anterior laminar surface. For the intraclass correlation coefficient, the I score at 95% CI was $0.932 < ICC < 0.994$, showing a robust delineation and quantification procedure in the assessment of the laminar depth measurement.

Investigative Ophthalmology & Visual Science

Downloaded From: http://iovs.arvojournals.org/pdfaccess.ashx?url=/data/journals/iovs/935339/ on 07/31/2017

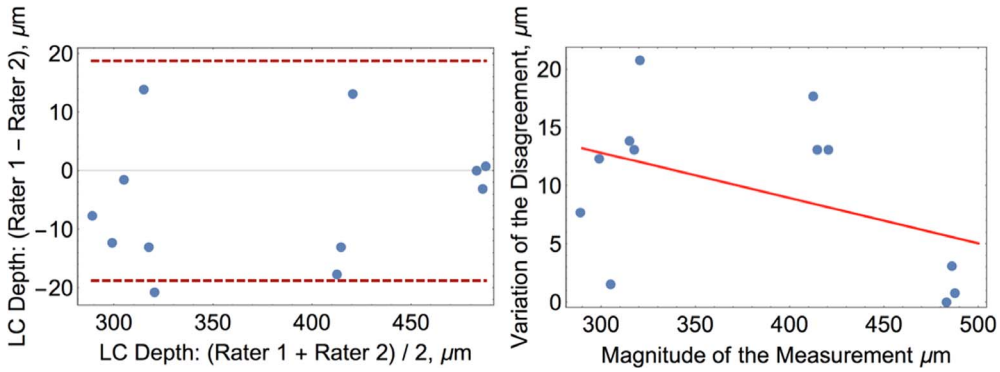

FIGURE 3. Bland-Altman plot for the interrater variability assessment. Disagreement in the estimate of the mean laminar depth (LC Depth) against the mean value estimated by the two raters is reported in the left plot. *Dashed line* = 95% CI. The right plot reports the association between magnitude of the disagreement and measurement magnitude computed as suggested by the authors in Altam et al.[35] and it shows a correlation of the two quantitates of 0.62.

Statistical Analysis

Generalized estimating equations (GEEs) accounting for the correlation among fellow eyes from the same individual were used in multivariate models where the response variables were the change in depth of the LC and PLT. Only covariates that showed a significant association with the response variables were used in the multivariate model. Probability values less than 0.05 were considered statistically significant.

Jackknife resampling and bootstrapping were used to assess the dependency of the outcomes from high leverage data points and the sample size.

Statistical analyses were performed using the R software (R Foundation for Statistical Computing, Vienna, Austria).

RESULTS

Demographic and ocular characteristics from the enrolled patients in each racial group are illustrated in Table 1. The African descent group was significantly younger than the ED group (Table 1). Thus, age was accounted as a continuous variable when found significantly associated with the response variable. The African descent group had significantly thinner CCT than the ED groups ($P = 0.0086$, Table 1); AL and ORA parameters were similar across racial groups. The ophthalmodynamometry-induced IOP elevation was on average 13.5 ± 4.9 mm Hg, but it varied with race (Fig. 2); the average increase in IOP in the ED group was 11.5 mm Hg, which was significantly lower than in the AD group 15 mm Hg, $P = 0.0235$. After 5 minutes from the ophthalmodynamometry compression, IOP dropped from a baseline of 18.5 mm Hg to 15.1 mm Hg, $P < 0.001$; IOP at 5 minutes was not significantly different between ED and AD, $P = 0.526$ (Table 1). Scatterplots of relevant covariates that showed significant correlations with change in laminar position in response to IOP are shown in Figure 4. In agreement with published studies,[36] BMO area was 22% larger in the AD group ($P < 0.001$), but despite this morphological difference the variation of the BMO area with IOP was not significant for either groups, nor was correlated with laminar displacement. Furthermore, laminar visibility was not significantly different ($P = 0.51$) with race or as a consequence of the IOP elevation ($P = 0.92$), as shown in Figure 5.

There was no significant association between age or Bruch's membrane opening and the ALCS displacement. For each millimeter of AL increase above the average, there was an associated increase in the ALCS posterior displacement of 10.44 μm ($P = 0.0169$, Fig. 4c). Increasing corneal resistance factor (7.58 μm/μm, $P = 0.0078$), CCT (0.26 μm/mm Hg , $P = 0.0137$), and CH (5.47 μm/mm Hg, $P = 0.020$) were all significantly positively associated with a deeper posterior displacement of the LC. Corneal resistance factor, CH, and CCT were highly correlated (Pearson correlation coefficient: CCT/CH 0.617; CCT/CRF 0.534; CH/CRF 0.768); hence in order to avoid multicollinearity effects only one of three corneal parameters was used as a covariate in the multivariable model. The corneal resistance factor was chosen based on an assessment of the goodness of fitting gaged by the Akaike information criterion score.

The results of the multivariable model for the amount of anterior laminar surface depth change and PLT across racial groups are shown in Table 2. Adjusted for age, AL, CRF, and the actual Δ IOP, the LC in the ED group showed a significant anterior displacement (–9.75 μm; $P = 0.0149$) compared to AD (19 μm; $P = 0.0092$). In the ED group, the ALCS displaced anteriorly (–3.34 μm/mm Hg; $P = 0.01$) in response to increased IOP. The African descent group showed a significantly different response than the ED group ($P = 0.0207$; Table 2) with a greater posterior displacement of the ALCS, as shown in Figure 4a.

While PLT strongly correlated with changes in the underlying laminar surface ($P < 0.001$, SE = 0.012; Table 2; Fig. 4d), the change in PLT did not reach statistical significance across racial groups ($P = 0.064$) or vary with AL ($P = 0.99$). There were similar independent associations seen between PLT with the change in IOP and the IOP at baseline (Table 2).

TABLE 1. Demographic and Ocular Characteristics Across AD and ED Groups

	Age, y	Sex	AL, mm	IOP Pre, mm Hg	Δ IOP, mm Hg	IOP Post, mm Hg	CCT, μm	CH, mm Hg	CRF, mm Hg
ED	55.8	10F/2M	23.6	18.5	11.6	15.6	557.6	10.48	10.98
AD	45.2	2F/7M	23.6	18.4	15.0	14.7	525.1	9.66	10.21
P value	0.065	NA	0.954	0.907	0.0235	0.526	0.0086	0.173	0.164

Investigative Ophthalmology & Visual Science

Downloaded From: http://iovs.arvojournals.org/pdfaccess.ashx?url=/data/journals/iovs/935339/ on 07/31/2017

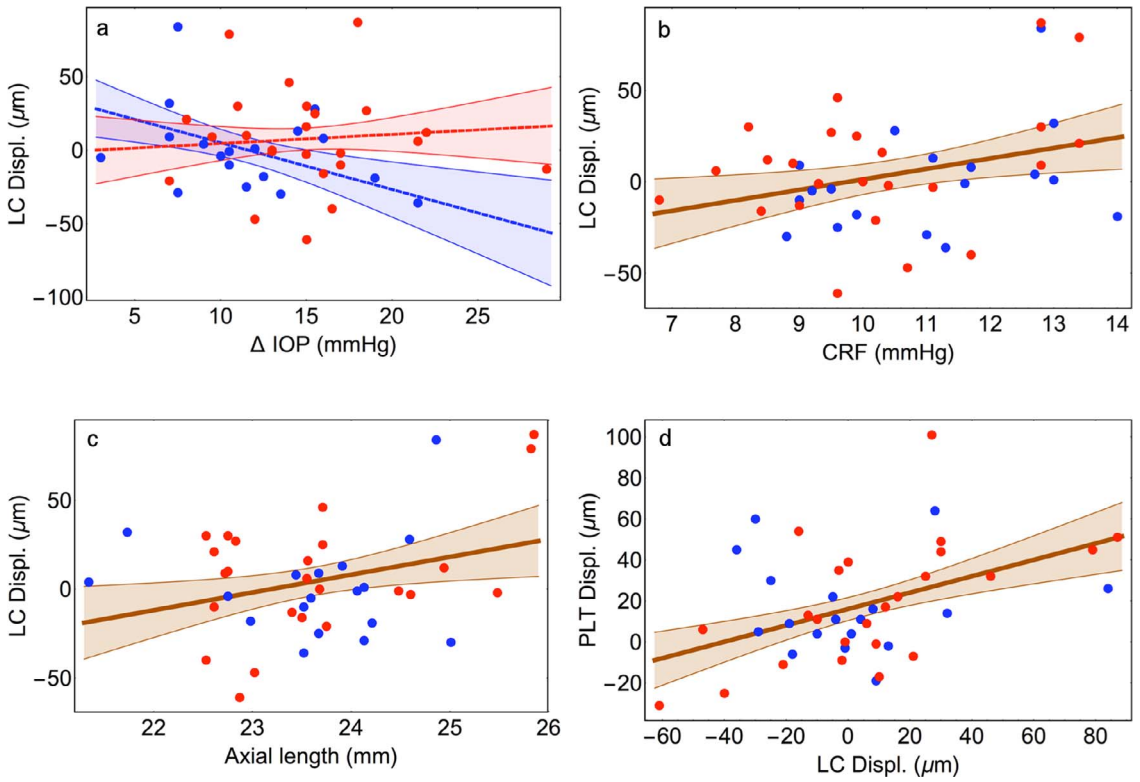

Figure 4. Scatterplots, regression line, and 95% CIs of the following outcomes: (**a**) anterior lamina cribrosa surface displacement (LC Displ.) resulted negatively correlated to an increase of IOP increase (Δ IOP) in the ED group (*blue*); the AD group (*red*) showed a inverse response to Δ IOP compared to EDs ($P = 0.0207$) consisting in a posterior displacement of the LC with increasing IOP. CIs bundle plotted in orange. (**b**) LC displ. was positively associated to CRF; the association did not show significant differences with race; (**c**) LC displ. regression with AL; in longer eyes the LC displaced significantly more posteriorly (0.0169). (**d**) The prelaminar tissue (PLT) tightly followed the direction of the LC displ. ($P < 0.001$); the effect was not found different in the racial strata.

Discussion

The results of this study suggest that the direction and magnitude of displacement of the lamina cribrosa following acute elevation of IOP is dependent with the magnitude of the IOP increase, differences in AL, corneal thickness and ORA parameters, and race (AD and ED). Specifically, after adjusting for the magnitude of the IOP increase, greater posterior displacement of the lamina cribrosa was associated with longer AL, thicker and stiffer (higher CH, and CRF) corneas, and in individuals of AD. These results are consistent with published computational modeling studies,[37–39] in addition to experimental in vivo and ex vivo studies of the human optic nerve head and peripapillary sclera as reviewed below.

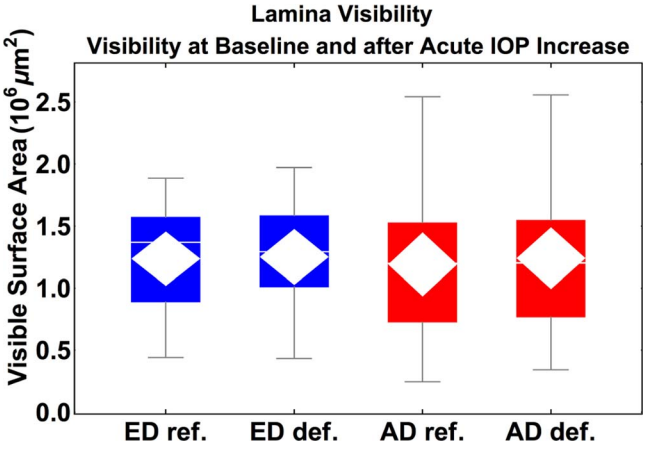

Figure 5. Difference in the visible anterior surface area before (reference, ref.) and after acute pressure elevation (deformed, def.) for the ED and AD groups. Lamina visibility did not show a significant association across racial strata and IOP increase, $P = 0.51$.

Table 2. Multivariable Model of the Average Anterior Laminar Surface (LC Displ.) and PLT Displacement (PLT Displ.) Following the Acute IOP Elevation

LC Displ.	Unit	Estimate	SE	*P* Value
ED	μm	−9.75	4.00	0.0149
AD	μm	19.0	7.30	0.0092
Δ IOP–ED	μm/mm Hg	−3.34	1.30	0.0100
Δ IOP–AD	μm/mm Hg	3.92	1.69	0.0207
Δ AL	μm/mm	10.44	4.37	0.0169
Δ CRF	μm/mm Hg	7.58	2.85	0.0078
PLT Displ.	**Unit**	**Estimate**	**SE**	***P* Value**
Intercept	μm	22.558	3.913	<0.001
LC depth	μm/μm	0.401	0.120	<0.001
Δ IOP	μm/mm Hg	3.399	0.625	<0.001
Δ IOP baseline	μm/mm Hg	3.269	0.858	<0.001

Estimates for the AD group indicate the magnitude of difference from the ED group, used as a control. Positive quantities indicate a posterior displacement (deepening in the canal) of the anterior lamina cribrosa surface, negative anterior. Δ, estimated change (delta); LC depth, lamina cribrosa depth (average).

Investigative Ophthalmology & Visual Science

Downloaded From: http://iovs.arvojournals.org/pdfaccess.ashx?url=/data/journals/iovs/935339/ on 07/31/2017

This finding of both anterior and posterior displacement of the lamina cribrosa following an increase in IOP can be mechanistically understood by considering two counterbalancing forces that impact the optic nerve region, the out-of-plane compression caused by the IOP, and in-plane stretching caused by the canal border displacement. Using numerical simulations, Sigal and coworkers[37,40] estimated that the direction of the laminar surface displacement was tightly dependent of the mechanical rigidity of the sclera and lamina cribrosa, in addition to laminar thickness. In these computational models, it was shown that the direction of deformation of the lamina was primarily regulated by peripapillary sclera rigidity. Indeed, for the same magnitude of IOP increase, in an eye with a more rigid sclera it was associated with a posterior deformation of the lamina, while in an eye with a more compliant peripapillary sclera it was associated with an anteriorization (shallowing) of the lamina.

This mechanism of deformation can be easily understood by looing at the lamina as a deformable membrane structure anchored to the ONH canal borders and subject to two opposing hydrostatic forces that are the IOP and the cerebrospinal fluid pressure. These forces create a direct translaminar pressure gradient that engenders posterior laminar displacement. Along with these out-of-plane forces, the canal enlargement creates a third in-plane (membrane) force that will instead draw the lamina cribrosa taut and pull anteriorly.

For example, in a compliant eye, an increase of IOP will likely generate an enlargement of the canal that will increase the in-plane strain of the lamina, flattening it. On the opposite side, a more rigid peripapillary sclera will allow only a small enlargement of the ONH canal, resulting in an in-plane tensile strain in the lamina that will not be enough to counterbalance the increase of hydrostatic pressure above the laminar surface; consequentially, a posterior bowing of the lamina will be observed. The interplay between these in-plane and out-of-plane forces sets the biomechanical behavior of the laminar microenvironment. Indeed, anterior migration of the lamina cribrosa has also been demonstrated in human glaucoma in an ED population.[41]

Considering these complex interactions, the greater posterior displacement in the AD group observed in the current study is in agreement with previous works from our group showing increased scleral stiffness in normal eyes from AD donors discussed below.[24,25] Fazio et al.[25] have published experimental results using laser electronic speckle pattern interferometry (ESPI) to quantify the displacement field in mechanical inflation testing of the posterior pole in normal human donor eyes. With this approach, we demonstrated that there is age-related stiffening of the peripapillary sclera,[42] that these changes occur most dramatically in regions of the ONH[43] known to be susceptible to glaucoma, and that these age-related changes differ significantly across AD and ED groups.[25] Grytz et al.[39] showed that a stiffer ring of collagen fibrils around the scleral canal promotes posterior displacements of the lamina cribrosa while reducing scleral canal expansion. Recently, we have shown that the peripapillary sclera is stiffer and stiffens more rapidly with IOP in donors of AD compared to ED, due to a higher shear stiffness and a lower level of stretch at which the collagen fibrils uncrimp. Consequently, the greater posterior displacement in patients of AD may be due to a stiffer peripapillary sclera in this racial subpopulation. The stiffer peripapillary sclera may be, in part, due to the higher percentage of occurrence of meridional fibers that Yan et al.[23] found in AD donors when compared to ED donors. A stiffer peripapillary sclera would inhibit the canal expansion to increasing IOP and promote the larger posterior displacement of the PLT that was found associated with higher baseline IOP, as peripapillary sclera stiffens nonlinearly with increasing IOP.[24,44] Unfortunately, the currently poor visibility in OCT images of the scleral tissue does not permit direct observation of the canal response to the IOP changes.

Furthermore, Coudrillier et al.[45] estimated that a stiffer sclera is associated with glaucomatous eyes. The same authors also showed that biomechanics of the peripapillary sclera is directly linked to the deformability of the ONH region.[45] These age-related changes and racial differences in scleral material properties and mechanical behavior likely play a critical role in modulating acute strain within the lamina cribrosa that is thought to be important in strain-mediated laminar remodeling in glaucoma.

Greater posterior displacement of the lamina cribrosa in the AD group is also consistent with our previous findings in vivo that there is an anterior shift in the laminar surface associated with aging in ED, but not AD normals.[19] These differential aging effects could reflect the impact of remodeling due to racial variation in acute strain within the lamina and peripapillary sclera suggested in the current in vivo study. In the current study, the laminar position also shifted anteriorly with acute IOP elevation prominently in the ED group (–9.8 μm, $P = 0.0149$; Table 2; Fig. 4a). These data suggest that the AD group may experience a proportionally greater translaminar strain compared to membrane strain than the ED group, which would result in greater posterior rather than anterior displacement and may have an impact on long-term age-related remodeling of these load bearing tissues.

The relationship between CCT, CH, and CRF with laminar displacement can also be understood within the context of this model. A thicker or stiffer cornea could correspond to a stiffer and thicker (more rigid) sclera; hence for the same increase of IOP the lamina would more likely be displaced posteriorly than stretched because of the reduced enlargement of the ONH canal in stiffer sclera. However, the relationship between the morphology and material properties of the cornea and the posterior sclera and optic nerve, while hypothesized,[46] has not been clearly demonstrated experimentally. It is very important to notice that many factors seem to affect the laminar displacement. Interestingly, the three eyes in Figure 4a that show a very large deepening of the lamina indeed have at the same time a very high CRF (stiff eye) and long AL (thinner lamina).

The positive correlation between AL and posterior deformation for the lamina is less intuitive. A plausible explanation of this association could be suggested by the negative correlation between laminar thickness and AL found in normal and glaucomatous individuals.[47] A thinner lamina would be more compliant to the direct effect of increased IOP than a thicker lamina, and this could explain why with an increase of AL we observe a more posterior displacement of the lamina (Fig. 4c).

Agoumi et al.,[22] using an approach similar to ours to evaluate how shifts in laminar position differed between a group of 12 patients with open angle glaucoma and 12 age-matched controls, found that while overall there was minimal difference in the means for laminar surface position at high and low IOP, there was a range of anterior and posterior shifts in response to IOP increase. These findings did not show a difference between glaucomatous and normal eyes, which was not evaluated in the current study; however, the study participants were all of ED, only four best corresponding scans at baseline and during IOP elevation were used for quantification of the morphological parameters, and EDI method was not available at the time of the study.

This is still consistent with our results in that overt posterior deformation was prominently seen in the AD group. Furthermore, we employed a 3D delineation system that allows

Investigative Ophthalmology & Visual Science

Downloaded From: http://iovs.arvojournals.org/pdfaccess.ashx?url=/data/journals/iovs/935339/ on 07/31/2017

for visualization and quantification of the entire visualizable lamina cribrosa rather than using a few selected b-scans. Also the 3D approach mitigates laminar depth quantification errors arising form the misalignments between the low- and high-pressure b-scans. Indeed, it is important to consider that the scan-points that lie in each b-scan of the low-pressure OCT acquisition do not necessarily lie in a plane after the IOP-induced morphological deformations.

The current study has several limitations. The measurement of IOP during pressure elevation, while immediately preceding imaging, is not simultaneous to the OCT acquisition. Since the force was manually applied, there could be some variation in IOP between when IOP is measured and the OCT image is obtained. A force feedback approach would be more optimal. However, any effect would likely be nondifferential across racial groups and consistent IOP could be maintained easily for over 60 seconds in our preliminary testing using the ophthalmodynamometry.

In order to minimize testing time for the enrolled individuals, in this study we set the in-between low- and high-pressure OCT scans waiting time to 60 seconds, under the assumption that the viscoelastic response of the lamina and peripapillary sclera lay in the same temporal order of magnitude. To the best of our knowledge, there is no available data that allow quantifying the time-scale of viscosity effects on the ONH deformation. Empirically, we know that the deformations of the peripapillary sclera following an ex-vivo acute pressure elevation "stabilizes" after a range of 5 to 20 seconds. Peripapillary sclera deformations are certainly linked to laminar deformation, but we do not know to what extent the viscoelastic properties of these tissues are alike. It is plausible that viscoelastic properties of the lamina differ across races and this could affect the magnitude of displacement; despite that a racial difference of the viscoelastic properties of the ONH region could not cause the opposite laminar displacement directions observed in the two groups.

The anterior lamina cribrosa surface could be only delineated in areas where its superior surface was clearly visible. Laminar visibility is affected by several factors; the most influential factors are the presence of shadowing retinal vessels and other individual-specific morphological features (thick PLT) that can rapidly weaken the OCT signal. It is important to notice that laminar visibility can affect the sampling region and this can cause a bias in the estimate of the laminar depth, although, our custom resampling approach was developed to minimize this bias. That considered, laminar visibility was not different for the two racial groups, neither changed after IOP elevation, as shown in Figure 5. Furthermore, it is important to keep in mind that the objective of this study is not the assessment of the actual laminar depth but its variation following an IOP increase, in the same eye. Moreover, the main outcome of this study is the observation in the two racial groups of an inverse trend in laminar direction of deformation, and there is no plausible explanation of how laminar visibility could oppositely bias the direction of laminar displacement in the two groups.

On the statistical model, we included all the measurable parameters that showed a significant association with laminar depth displacement, but we are certain that other influential factors that are not currently measured in this study have a significant influence on the laminar depth displacement. For example, the morphology of the canal is likely a very important biomechanical influential parameter for lamina deformation, but the current OCT technology does not allow an accurate estimate of that region. Interestingly, disk size (BMO area) did not show a significant association with the change in laminar depth, suggesting that this parameter is not a biomechanical surrogate for the canal size.

The current linear regression model cannot provide an estimate of the lamina cribrosa surface displacement to small IOP increases. Considering that at zero Δ IOP the LC displacement should be zero, the actual functional relation between LC displacement and increase of IOP (LC Displ. versus Δ IOP; Fig. 4a) is likely a high-degree nonmonotonic curve whose statistical modeling would require a much larger number of observations at lower IOP than those available in this study. Ideally, a larger set of data points associated with low Δ IOP values would allow an estimate of the regression shape close to the zero pressure increase point. It is very important to notice that while age, CRF, and AL vary cross-sectionally among individuals, the lamina cribrosa displacement is longitudinally measured in the same eye, so each laminar depth change is computed against its internal control.

In summary, we demonstrated that there was greater posterior deformation in the lamina cribrosa in AD compared to ED normal individuals in response to an acute increase of IOP. This significant variation in laminar compliance across racial groups may be related to described differences in the morphometric and material properties of the ONH region and could explain some of the differential susceptibility to glaucomatous injury in the at-risk AD population. Dedicated studies are needed to determine if longitudinal variations in compliance of the lamina cribrosa are associated with the development and progression of glaucoma and how compliance changes over time with the disease.

Acknowledgments

The authors thank Claude Burgoyne, MD, for providing the *Multiview* delineation software used in this study.

Supported by Research to Prevent Blindness (RPB), and the Eyesight Foundation of Alabama (ESFA).

Disclosure: **M.A. Fazio**, None; **J.K. Johnstone**, None; **B. Smith**, None; **L. Wang**, None; **C.A. Girkin**, None

References

1. Roberts MD, Liang Y, Sigal IA, et al. Correlation between local stress and strain and lamina cribrosa connective tissue volume fraction in normal monkey eyes. *Invest Ophthalmol Vis Sci*. 2010;51:295–307.
2. Yang H, Thompson H, Roberts MD, Sigal IA, Downs JC, Burgoyne CF. Deformation of the early glaucomatous monkey optic nerve head connective tissue after acute IOP elevation in 3-D histomorphometric reconstructions. *Invest Ophthalmol Vis Sci*. 2011;52:345–363.
3. Burgoyne CF, Downs JC, Bellezza AJ, Suh JK, Hart RT. The optic nerve head as a biomechanical structure: a new paradigm for understanding the role of IOP-related stress and strain in the pathophysiology of glaucomatous optic nerve head damage. *Prog Retin Eye Res*. 2005;24:39–73.
4. Burgoyne CF, Downs JC. Premise and prediction—how optic nerve head biomechanics underlies the susceptibility and clinical behavior of the aged optic nerve head. *J Glaucoma*. 2008;17:318–328.
5. Nguyen C, Cone FE, Nguyen TD, et al. Studies of scleral biomechanical behavior related to susceptibility for retinal ganglion cell loss in experimental mouse glaucoma. *Invest Ophthalmol Vis Sci*. 2013;54:1767–1780.
6. Quigley H, Addicks E, Green W, Maumenee A. Optic nerve damage in human glaucoma. II. The site of injury and susceptibility to damage. *Arch Ophthalmol*. 1981;99:635–649.
7. Quigley HA, Addicks EM. Chronic experimental glaucoma in primates. II. Effect of extended intraocular pressure elevation

Investigative Ophthalmology & Visual Science

Downloaded From: http://iovs.arvojournals.org/pdfaccess.ashx?url=/data/journals/iovs/935339/ on 07/31/2017

on optic nerve head and axonal transport. *Invest Ophthalmol Vis Sci*. 1980;19:137–152.

8. Sigal IA, Grimm JL, Jan N-J, Reid K, Minckler DS, Brown DJ. Eye-specific IOP-induced displacements and deformations of human lamina cribrosa. *Invest Ophthalmol Vis Sci*. 2014;55:1–15.
9. Downs JC. Optic nerve head biomechanics in aging and disease. *Exp Eye Res*. 2015;133:19–29.
10. Burgoyne CF, Morrison JC. The anatomy and pathophysiology of the optic nerve head in glaucoma. *J Glaucoma*. 2001;10:S16–S18.
11. Quigley HA, Cone FE. Development of diagnostic and treatment strategies for glaucoma through understanding and modification of scleral and lamina cribrosa connective tissue. *Cell Tissue Res*. 2013;353:231–244.
12. Quigley HA, Addicks EM, Green WR, Maumenee AE. Optic nerve damage in human glaucoma. II. The site of injury and susceptibility to damage. *Arch Ophthalmol*. 1981;99:635–649.
13. Spaide RF, Koizumi H, Pozonni MC. Enhanced depth imaging spectral-domain optical coherence tomography. *Am J Ophthalmol*. 2008;146:496–500.
14. Girard MJ, Strouthidis NG, Ethier CR, Mari JM. Shadow removal and contrast enhancement in optical coherence tomography images of the human optic nerve head. *Invest Ophthalmol Vis Sci*. 2011;52:7738–7748.
15. Vermeer KA, Mo J, Weda JJA, Lemij HG, de Boer JF. Depth-resolved model-based reconstruction of attenuation coefficients in optical coherence tomography. *Biomed Opt Express*. 2014;5:322–337.
16. Girard MJA, Tun TA, Husain R, et al. Lamina cribrosa visibility using optical coherence tomography: comparison of devices and effects of image enhancement techniques. *Invest Ophthalmol Vis Sci*. 2015;56:865–874.
17. Ren R, Yang H, Gardiner SK, et al. Anterior lamina cribrosa surface depth, age, and visual field sensitivity in the Portland progression project. *Invest Ophthalmol Vis Sci*. 2014;55:1531–1539.
18. Park SC, Brumm J, Furlanetto RL, et al. Lamina cribrosa depth in different stages of glaucoma. *Invest Ophthalmol Vis Sci*. 2015;56:2059–2064.
19. Rhodes LA, Huisingh C, Johnstone J, et al. Variation of laminar depth in normal eyes with age and race. *Invest Ophthalmol Vis Sci*. 2014;55:8123–8133.
20. Strouthidis NG, Fortune B, Yang H, Sigal IA, Burgoyne CF. Effect of acute intraocular pressure elevation on the monkey optic nerve head as detected by spectral domain optical coherence tomography. *Invest Ophthalmol Vis Sci*. 2011;52:9431–9437.
21. Jiang R, Xu L, Liu X, Chen JD, Jonas JB, Wang YX. Optic nerve head changes after short-term intraocular pressure elevation in acute primary angle-closure suspects. *Ophthalmology*. 2015;122:730–737.
22. Agoumi Y, Sharpe GP, Hutchison DM, Nicolela MT, Artes PH, Chauhan BC. Laminar and prelaminar tissue displacement during intraocular pressure elevation in glaucoma patients and healthy controls. *Ophthalmology*. 2011;118:52–59.
23. Yan D, McPheeters S, Johnson G, Utzinger U, Vande Geest JP. Microstructural differences in the human posterior sclera as a function of age and race. *Invest Ophthalmol Vis Sci*. 2011;52:821–829.
24. Grytz R, Fazio MA, Libertiaux V, et al. Age- and race-related differences in human scleral material properties. *Invest Ophthalmol Vis Sci*. 2014;55:8163–8172.
25. Fazio MA, Grytz R, Morris JS, Bruno L, Girkin CA, Downs JC. Human scleral structural stiffness increases more rapidly with age in donors of African descent compared to donors of European descent. *Invest Ophthalmol Vis Sci*. 2014;55:7189–7198.
26. Sample PA, Girkin CA, Zangwill LM, et al. The African Descent and Glaucoma Evaluation Study (ADAGES): design and baseline data. *Arch Ophthalmol*. 2009;127:1136–1145.
27. Racette L, Liebmann JM, Girkin CA, et al. African Descent and Glaucoma Evaluation Study (ADAGES): III. Ancestry differences in visual function in healthy eyes. *Arch Ophthalmol*. 2010;128:551–559.
28. Lee EJ, Kim TW, Weinreb RN, Park KH, Kim SH, Kim DM. Visualization of the lamina cribrosa using enhanced depth imaging spectral-domain optical coherence tomography. *Am J Ophthalmology*. 2011;152:87–95.
29. Girard MJSN, Ethier CR, Mari JM. Shadow removal and contrast enhancement in optical coherence tomography images of the human optic nerve head. *Invest Ophthalmol Vis Sci*. 2011;52:7738–7748.
30. Mari JM, Strouthidis NG, Park SC, Girard MJ. Enhancement of lamina cribrosa visibility in optical coherence tomography images using adaptive compensation. *Invest Ophthalmol Vis Sci*. 2013;54:2238–2247.
31. Downs JC, Yang H, Girkin CA, et al. Three-dimensional histomorphometry of the normal and early glaucomatous monkey optic nerve head: neural canal and subarachnoid space architecture. *Invest Ophthalmol Vis Sci*. 2007;48:3195–3208.
32. Strouthidis NG, Yang H, Downs JC, Burgoyne CF. Comparison of clinical and three-dimensional histomorphometric optic disc margin anatomy. *Invest Ophthalmol Vis Sci*. 2009;50:2165–2174.
33. Johnstone J, Fazio M, Rojananuangnit K, et al. Variation of the axial location of Bruch's membrane opening with age, choroidal thickness, and race. *Invest Ophthalmol Vis Sci*. 2014;55:2004–2009.
34. Song Q, Bai J, Garvin MK, Sonka M, Buatti JM, Wu X. Optimal multiple surface segmentation with shape and context priors. *IEEE Trans Med Imaging*. 2013;32:376–386.
35. Altman DG, Bland JM. Measurement in medicine: the analysis of method comparison studies. *J Royal Stat Soc Series D (The Statistician)*. 1983;32:307–317.
36. Lee RY, Kao AA, Kasuga T, et al. Ethnic variation in optic disc size by fundus photography. *Curr Eye Res*. 2013;38:1142–1147.
37. Sigal IA, Yang H, Roberts MD, Burgoyne CF, Downs JC. IOP-induced lamina cribrosa displacement and scleral canal expansion: an analysis of factor interactions using parameterized eye-specific models. *Invest Ophthalmol Vis Sci*. 2011;52:1896–1907.
38. Sigal IA, Flanagan JG, Ethier CR. Factors influencing optic nerve head biomechanics. *Invest Ophthalmol Vis Sci*. 2005;46:4189–4199.
39. Grytz R, Meschke G, Jonas J. The collagen fibril architecture in the lamina cribrosa and peripapillary sclera predicted by a computational remodeling approach. *Biomech Model Mechanobiol*. 2011;10:371–382.
40. Sigal IA, Ethier CR. Biomechanics of the optic nerve head. *Exp Eye Res*. 2009;88:799–807.
41. Wu Z, Xu G, Weinreb RN, Yu M, Leung CK. Optic nerve head deformation in glaucoma: a prospective analysis of optic nerve head surface and lamina cribrosa surface displacement. *Ophthalmology*. 2015;122:1317–1329.
42. Fazio MA, Grytz R, Morris JS, et al. Age-related changes in human peripapillary scleral strain. *Biomechan Modeling Mechanobiol*. 2013;13:551–563.
43. Fazio MA, Grytz R, Bruno L, et al. Regional variations in mechanical strain in the posterior human sclera. *Invest Ophthalmol Vis Sci*. 2012;53:5326–5333.
44. Girard MJ, Downs JC, Bottlang M, Burgoyne CF, Suh JK. Peripapillary and posterior scleral mechanics–part II: experi-

Investigative Ophthalmology & Visual Science

Downloaded From: http://iovs.arvojournals.org/pdfaccess.ashx?url=/data/journals/iovs/935339/ on 07/31/2017

mental and inverse finite element characterization. *J Biomech Engin*. 2009;131:051012.

45. Coudrillier B, Boote C, Quigley H, Nguyen T. Scleral anisotropy and its effects on the mechanical response of the optic nerve head. *Biomech Model Mechanobiol*. 2013;12:941–963.
46. Lee E, Kim T-W, Weinreb R, Suh M, Kim H. Lamina cribrosa thickness is not correlated with central corneal thickness or axial length in healthy eyes. *Graefe's Arch Clin Exp Ophthalmol*. 2013;251:847–854.
47. Ren R, Wang N, Li B, et al. Lamina cribrosa and peripapillary sclera histomorphometry in normal and advanced glaucomatous Chinese eyes with various axial length. *Invest Ophthalmol Vis Sci*. 2009;50:2175–2184.

Investigative Ophthalmology & Visual Science

Downloaded From: http://iovs.arvojournals.org/pdfaccess.ashx?url=/data/journals/iovs/935339/ on 07/31/2017